This is a peer-reviewed, accepted author manuscript of the following article: Tauanov, Z., Shah, D., Inglezakis, V., & Jamwal, P. K. (2018). Hydrothermal synthesis of zeolite production from coal fly ash: a heuristic approach and its optimization for system identification of conversion. *Journal of Cleaner Production*, *182*, 616-623. https://doi.org/10.1016/j.jclepro.2018.02.047

Hydrothermal synthesis of zeolite production from coal fly ash: A heuristic approach and its optimization for system identification of conversion

Zhandos Tauanov[1], Dhawal Shah[1,*], Vassilis Inglezakis[1], and Prashant K. Jamwal[2]

[1]Department of Chemical Engineering, Environmental Science & Technology Group (ESTg), School of Engineering, Nazarbayev University, Kazakhstan
[2]Department of Electrical Engineering, School of Engineering, Nazarbayev University, Kazakhstan

*Corresponding author: dhawal.shah@nu.edu.kz

Keywords: Zeolites, Hydrothermal production, heuristic methods, Coal Fly Ash

Highlights:

1. Production of synthetic zeolites derived from coal fly ash
2. Effect of the process parameters on conversion into zeolites
3. Heuristic approach of production optimization
4. Fuzzy modeling as an effective system architecture

Abstract

With growing interest in commercialization of synthetic zeolites, impetus is on the optimization of its production process. This, however, requires a thorough understanding of the zeolitization process and apropos reaction mechanism(s). The preferred commercial production route for synthesis of zeolites is hydrothermal treatment of coal fly ash in a strong alkali solution at elevated temperatures. The process involves several parameters, such as reaction temperature, time, the concentration and amount of alkali solution, and silica content in the fly ash, which strongly affect the conversion. These parameters appear to have an arbitrary effect on the yield of zeolite. In order to gain insights into the process and thereby, the reaction mechanism(s), we herein propose a conversion model using zero-order Takagi-Sugeno fuzzy system and optimize it further. The model is designed and developed, using the data, both from literature and our experiments, and is later optimized to provide accurate inferences. Results clearly illustrate that the model is able to accurately predict the conversion percentage of zeolite for a given set of reaction parameters. Average deviation between the model predictions and experimental values for zeolite yield is observed to be less than 5%. Moreover, the model also assists in characterizing the dependence of conversion on individual parameters, which further sheds light on the mechanism(s) of zeolite formation.

Introduction

Environmental Protection Agency estimates a discharge of coal fly ash (CFA), a by-product from combustion of coal in electric power stations, to as high as 140 million tons per year. Considering the huge quantities of CFA generated and the fact that it causes serious environmental and health problems [1-3], further investigation on the management of CFA is essential. One of the efficient ways of converting CFA into a value-added product is producing synthetic zeolites [4-7], which have a wide range of application, particularly in the field of agricultural, pollution treatment, and catalysis [8]. While synthetic zeolites can also be produced using various raw materials as clay minerals [9-11] and siliceous minerals [12], CFA is considered as suitable stock material due to its negligible cost, abundant availability, and possibility to produce different zeolites by altering reaction conditions [13]. The chemical composition of zeolite and CFA is almost the same; however, these two differ in their crystallinity: CFA is mainly composed of amorphous structure, while zeolite has a well-defined crystalline structure [16]. In addition, zeolite has higher cation exchange capacity (CEC), larger surface area, and also demonstrates superior thermal stability [17] than CFA and hence further enhances utilization sectors.

Immense interest has been shown by industries for commercializing the process to convert CFA. Following the interest, over the past decades, there have been numerous studies on synthesis of zeolites from CFA on lab-, pilot-, and also on industrial-scale [13-15]. For example, Wdowin et al. [13] with their sub-pilot scale converted 20 kg of CFA to NaP1 zeolite with a purity of 81%. Similarly, studies also demonstrate economic feasibility to manufacture zeolitic adsorbents from coal fly ash thereby allowing its potential utilization [14, 15]. There are several existing methods for production of zeolites from CFA, such as hydrothermal conversion using alkaline solutions [8, 16, 17], microwave-assisted [2], ultrasound-assisted [4, 18, 19], fusion followed by hydrothermal

synthesis [20-23], and salt-thermal production [24] process. However, hydrothermal synthesis, that is multiphase crystallization including both amorphous and crystalline solid phases and at least one liquid phase [25], is still the most promising and widely applied method. According to this method the raw coal fly ash is dissolved in alkaline solution, usually NaOH, to extract aluminate and silicate constituents, which then undergoes heat treatment to produce zeolite crystals [15, 26]. Despite the fact that there are numerous investigations that have already been recorded and published on hydrothermal synthesis of zeolites, the underlying mechanism of zeolite formation is not well understood and thus the production process are still not optimized.

There are several parameters that affect the zeolitization process, viz., alkali concentration, time, reaction temperature, loading ratio (volume of the alkali solution to weight of CFA, i.e, liquid to solid ratio, L/S), and Si/Al ratio in CFA [8, 16, 17, 27]. Depending on these conditions it is possible to obtain different purity and type of synthetic zeolites, such as zeolite A [6], zeolite Na-P [4], sodalite [28] etc. The available data in the literature on hydrothermal conversion of zeolites from CFA to emphasize the effect of process conditions on conversion efficiency are summarized in Table 1.

Table 1: Effect of process conditions on hydrothermal synthesis of synthetic zeolites from CFA.

#	Conc.[a] (M)	Time (h)	Temperature (°C)	L/S[b] (ml/g)	Si/Al	Zeolite type	Conv.[c] %	Ref.
1	1	24	80-130	2	1.29	NaP1	20	{d}
2	1	48	122-166	2	1.29	NaP1	60	{d}
3	1	48	126-192	2	1.29	NaP1/Analcime	80	{d}
4	1	48	100-130	2	1.29	NaP1/Analcime	75	{d}
5	2	24	92-114	1.25	1.29	NaP1/Analcime	75	{d}
6	2	24	100-110	1.25	1.29	NaP1	75	{d}
7	2	24	90-100	1.25	1.29	NaP1	75	{d}
8	2	48	80-130	1.25	1.29	NaP1	65	{d}
9	2	22	125-187	2	1.29	NaP1	60	{d}
10	2	72	120-190	2	1.29	NaP1/Analcime	80	{d}

11	2	72	130-160	2	1.29	NaP1/Analcime/chabazite	80	{d}
12	2	24	131-174	2.5	1.29	NaP1/Analcime	65	{d}
13	2	48	110-180	2.5	1.29	NaP1/Analcime	75	{d}
14	2	48	110-160	2.5	1.29	Analcime	60	{d}
15	1	24	90	20	1.44	NaP1	19.8	{e}
16	1	24	110	20	1.44	NaP1	45.3	{e}
17	1	48	90	20	1.44	NaP1	48.3	{e}
18	3	24	90	20	1.44	NaP1	39.6	{e}
19	1	48	110	20	1.44	NaP1	47	{e}
20	3	24	110	20	1.44	NaP1	55.9	{e}
21	3	48	90	20	1.44	NaP1	35.5	{e}
22	3	48	110	20	1.44	NaP1	78	{e}
23	0.5	24	150	18	2.9	NaP1/Analcime	44	{f}
24	1	24	150	18	2.9	NaP1/Analcime	50	{f}
25	0.5	24	150	18	2.7	NaP1/Analcime	44	{f}
26	3.5	24	150	18	2.7	Cancrinite/Sodalite/Z-X	21	{f}
27	1	24	150	18	2.7	NaP1/Analcime	60	{f}
28	2	24	100	18	2.7	NaP1	17	{f}
29	3	24	100	18	2.7	NaP1/Sodalite/Z-X	48	{f}
30	3.5	24	100	18	2.7	NaP1/Sodalite	35	{f}
31	3	24	75	20	1.88	Na-X	50	{g}

a: Concentration of alkali; **b**: volume of the alkali solution to weight of CFA; **c**: Total conversion of CFA to zeolite; irrespective of the type of zeolite formed; **d**: As reviewed by Wang et al. [29], **e**: Our experiments; details mentioned below, **f**: Experiments by Cardoso et al. [27], **g**: Experiments by Derkowski et al. [30].

Table 1 indicates strong, non-monotonic, and to some degree, random dependence of conversion on process conditions. For example, a slight change in loading ratio from 2 to 1.25 strongly increases conversion from 20% to 75% (see point 1 and 7). However, increasing the loading ratio to 18 brings conversion to 50% (see point 1 and 15). There are several other comparisons that can be done to highlight the random behavior. At this point, we also emphasize that the values reported in the literature are all experimentally determined and thus might be subjected to statistical errors but we presume that all the values are repeatable. In this reference, the experiments presented in this paper had maximum standard deviation of 5% for conversion. The details of experimentations are mentioned later.

In order to commercialize zeolitization of CFA, optimization of process conditions is essential to maximize the yield. The intricacy of the reaction mechanism(s) is too complicated to be analytically model, which is vital in order to optimize the zeolitization process. However, as shown above, the interdependence between the antecedents and the consequents of the process is quite uncertain, ambiguous and nonlinear. To the best of our knowledge, no theoretical or mathematical reaction model exists to explain or determine zeolite conversion from CFA. While conventional numerical and analytical modelling techniques may not emulate such processes with precision, there exist heuristic methods which can effectively modeled uncertain and ambiguous systems.

Fuzzy logic is one of such heuristic methods whereby the available quantitative data is converted into qualitative data and a logical inference is drawn using appropriately designed rule-base. In the present research, a fuzzy logic-based system is developed in order to identify and model the mechanism of zeolitization process. Building blocks of the proposed system and their development is further elaborated in the next section. We believe the method we propose will inherently assist in better understanding of zeolitization mechanism and in finding optimum reaction parameters, which correspondingly emphasizes the necessity for this type of research. We begin with details on experiments conducted to convert fly ash to zeolites followed by the architecture of the fuzzy system used.

Materials and Methodology

A representative coal fly ash (CFA) sample with a composition typical of the average CFA output was collected from the electrostatic precipitators of coal-fired power plant of Astana, Kazakhstan under maximum electricity load. All CFA samples were used as received without preliminary washing and sieving. Prior to experiment CFA samples were homogenized and dried in

oven at 70 °C for 12 h. The sodium hydroxide of analytical grade (Fischer Scientific, pearls, >97%) was used to prepare an alkaline solution with various concentrations.

To produce synthetic zeolite (ZFA), CFA underwent an alkaline hydrothermal treatment at 90-110°C, using NaOH with concentrations of 1 or 3 M as an activation solution, in a 1L heavy-walled glass reactor. The incubation period was set at 24 hours (unless specified otherwise) and a mixing rate was set constant at 125 rpm for all experiments. After set period, the mixture was filtered and washed several times until no NaOH was detected. The mineralogical compositions of the CFA and zeolites were determined by X-Ray Diffraction (XRD, Rigaku SmartLab) and the compositions were used to compute percentage conversion to zeolites. Factorial analysis was carried using three parameters, namely the reaction temperature, time, and alkali concentration, following which eight experiments were designed, as mentioned later in Table 4, to investigate the effects of the parameters on CFA on zeolite conversion.

Fuzzy system architecture

The proposed fuzzy logic based system is also known as Takagi-Sugeno (TS) fuzzy system which was first introduced by Takagi and Sugeno [31] and has been extensively used in diverse applications across disciplines. Essentially, there are three main building blocks which are required to be defined in developing a fuzzy based system. Fuzzification of antecedent and consequent variables is the first block while construction of a rule-base, describing the relationship between variables, is the second building block. Formulation of an inference mechanism to provide numerical values of output or consequent variables is the third building block of the fuzzy systems. The fuzzy system developed during this research is further explained in terms of these building blocks in the ensuing section.

Fuzzification: Fuzzification is the process whereby crisp antecedent and consequent variables are defined as fuzzy variables. In the present research there are five antecedent variables namely, molar concentration, temperature, time, mixture loading ratio (L/S), and Si/Al. The output variable is the percentage zeolite conversion (Conv.) from Table 1. First, we convert the antecedent variables into fuzzy variables using fuzzy sets. We choose the Gaussian distribution for the shape of the Activation Functions (AFs) since they provide smooth transition between AFs. Later, we decide on the number of AFs and their parameters such as mean and standard deviation. Number of AFs for i^{th} input (M_i), can be two or more depending on the accuracy of results required. However, we can automatically compute the points of minimum fuzziness (or center points of AFs shown by B & C in Figure 1) and standard deviations (σ_i) of AFs along with the range of variables (R_i) using extreme values (i.e. minimum and maximum) of variables (v_i) during execution of the algorithm using eq. (1-3).

$$R_i = (1.25 * \max(v_i) - 0.75 * \min(v_i)) \tag{1}$$

$$A_i = 0.75 * \min(v_i)\,;\; B_i = A_i + \frac{R_i}{(2M_i - 1)}; C_i = B_i + \frac{R_i}{(2M_i - 1)}; D_i = 1.25 * \max(v_i) \tag{2}$$

$$\sigma_i = R_i/(2 * (2M_i - 1)) \tag{3}$$

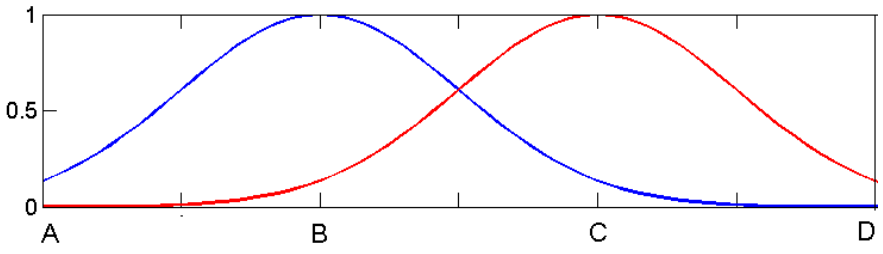

Figure 1: Minimum fuzziness points of a Gaussian AF

Heuristic models such as the one we discuss here can be assessed based on two parameters namely, interpretability and accuracy. Unfortunately, these two parameters are conversely related

and the designers normally have to trade off the accuracy for the sake of interpretability. Accordingly, in order to have better interpretability and avoid overfitting of data, the antecedent variables are all defined using only two AFs as shown in the Figure 2. The AFs, for the sake of discrimination, are named as Low (L) and High (H).

The consequent variables are not defined in the beginning rather these are obtained during the course of the algorithm. We obtained a set of real numbers for consequent variables while using a zero order TS fuzzy system. We are not considering higher order fuzzy systems in the present case, which provide polynomial functions for consequent variables, due to their non-linearity and subsequent higher complexity. We should also note that in Table 1, certain data points have range of values for temperature; and in such cases, an average value was used.

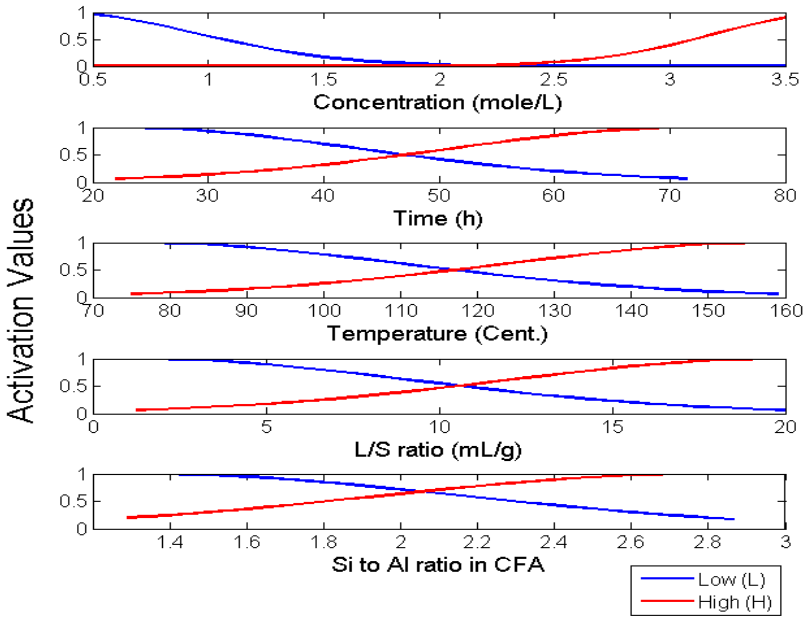

Figure 2: Fuzzification of antecedent variables of the fuzzy system

Rule-base Development: During design of fuzzy systems, development of a rule-base is an important task which requires expert knowledge and meticulous data analysis. The rule-base of a TS

fuzzy system relates the fuzzy antecedent and crisp consequent variables using *if-then statements* and has the following structure.

$$If conc.\, is\ low, time\ is\ high, \ldots\ldots\ldots then\ the\ output\ (CR) is\ y_i$$

Fundamentally, we derive the total number of rules (N_r) from the number of input variables (n) and AFs (m_k) using following relation.

$$N_r = \prod_{k=1}^{n} m_k \tag{4}$$

Therefore, in the present system where there are five input variables and each of these is defined using two AFs, the total number of rules in the rule-base is 2^5=32. Accordingly, the set of consequent variables shall also have 32 real numbers for the present zero order TS fuzzy system. We identify the consequent variables using the pseudo-inverse operator in the inference mechanism block as explained in the following Section.

Inference mechanism: In order to calculate output conversion of zeolite ($Conv.$) from the fuzzy model for given inputs, we compute weighted average from all the individual rules and multiply with the set of consequent variables. In fact, computation of output from the fuzzy model is a two-step procedure which is based on a weighted average defuzzifier [32]. Firstly, we evaluate degrees of fulfilment (w_i) for k^{th} input (I_k) from all the rules using (5-8). Here activations of input variables in 'Low' and 'High' AFs are given by $A_{kL}(I_k)$ and $A_{kH}(I_k)$ respectively and calculated using (5 & 6). Constant 'a' in the equations is given by 1/(σ√2π) while e denotes the Euler's number. The degrees of fulfilment (w_i) for i^{th} input from all the rules are calculated using a product operation (8). In the subsequent step we compute the final output ($Conv.$) using weighted average of the individual rule fulfilments using (9). P_{ik} is the selection vector which chooses the activation function to be used in input k and rule i.

$$A_{km}(I_k) = ae^{-\frac{(I_k - \bar{I}_{km})^2}{2\sigma_{km}}}; \qquad where \quad m = L, H \tag{5}$$

$$A_k(I_k) = [A_{kL}\ A_{kH}]^T \tag{7}$$

$$w_i = \prod_{k=1}^{5} P_{ik} A_k(I_k) \tag{8}$$

$$Conv. = \frac{\sum_{i=1}^{N_r}(w_i . y_i)}{\sum_{i=1}^{N_r} w_i} \tag{9}$$

In equation (9) above y_i is the vector of 32 consequent values which is required to be identified in order to compute the final output from the model. As explained above, this vector is also the consequent part of the rule-base. Apparently, (9) can be further rewritten as (10), with X being a regressor vector or a vector of normalized weights ($w_i/sum(w_i)$) coming from all the rules for a given set of inputs. Here W is the weight vector and it consists of the consequent parameters.

$$Conv. = X * W \tag{10}$$

Interestingly, when multiple observations (of inputs and corresponding outputs) are available from experiments, we can obtain the weight vector (W) using a regression technique. Normally, the regressor matrix is non invertible and therefore we use its pseudoinverse to solve for W (11).

$$W = X^{-1} * Conv. \tag{11}$$

$$W = (X^T * X)^{-1} * X^T * Conv. \tag{12}$$

Using (11 & 12) we can obtain a vector of consequent parameters which will minimize the error between the predicted $Conv.$ and the target $Conv.$ from experiments.

Optimization of fuzzy model

To begin with, we intuitively decide the parameters of fuzzy system such as mean and standard deviation of the fuzzy AFs. However, such a system may not accurately represent the zeolitization process and therefore fuzzy system parameters are required to be tuned in order to optimize the fuzzy model for enhanced accuracy. Or in other words, we need to optimize the fuzzy model in such a manner so that we minimize the prediction error from the model. Since, we tune the parameters within their limiting values; it is a constrained optimization problem which involves multiple variables which may be non-linear in nature. We use the available data (set of inputs and zeolite yield) to tune fuzzy parameters and produce the desired system model. Herein, we tune the fuzzy parameters by using a gradient descent algorithm which minimizes an objective error function (E) as described below.

Minimize

$$E = \frac{1}{N}\sum_{p=1}^{N}\left[\frac{1}{2}(|C_p| - |C_p^e|)^2\right] \tag{13}$$

Here, E is the expected value of the squared errors for the magnitude of zeolite yield while N stands for the total number of experimental observations. Further, we denote the output from the fuzzy model by C_p whereas C_p^e is the zeolite yield from p^{th} experiments for the same set of inputs. We propose zero order TS fuzzy model that has five inputs and each of these we define using two AFs (Figure 2), which means that the total number of AFs is 10. Further, we describe each of the Gaussian AF by two parameters namely, mean and standard deviation. Therefore, there are 20 parameters for the antecedent fuzzy variables which are required to be tuned.

Using gradient descent method, we can update the fuzzy parameters in order to minimize the objective error function (13). We can formulate the update rule for various parameters as (14).

$$p_{km}(t+1) = p_{km}(t) - \frac{\alpha}{N}\sum_{p=1}^{N}\frac{\partial E^p}{\partial p_{km}} \tag{14}$$

Here in equation (14), p_{km} is the vector of antecedent fuzzy AF parameters for k^{th} input and m^{th} AF. Number of epochs is given by 't', constant 'α' is used for the learning rate which usually decide the quantum of change in the parameters following every iteration and 'N' denotes the number of observations available for tuning. Partial derivatives for the parametric updates shown in (14) we can calculate using the following chain rule.

$$\frac{\partial E_p}{\partial p_{km}} = \sum_{p=1}^{N}\left(\frac{\partial E_p}{\partial C_p}\cdot\frac{\partial C_p}{\partial w_i^p}\cdot\frac{\partial w_i^p}{\partial A_{km}^p}\cdot\frac{\partial A_{km}^p}{\partial p_{km}}\right) \tag{15}$$

The partial derivatives in the chain rule we can further calculate as below.

$$\text{Since} \quad E_p = \frac{1}{2}(|C_p| - |C_p^e|)^2; \qquad \frac{\partial E_p}{\partial C_p} = (|C_p| - |C_p^e|) \tag{16}$$

$$\text{Further since} \quad C_p = \frac{\sum_{i=1}^{N_r}(w_i.y_i)}{\sum_{i=1}^{N_r} w_i}; \qquad \frac{\partial C_p}{\partial w_i^p} = \frac{(y_i^p - C_p)}{\sum_{i=1}^{N_r} w_i^p} \tag{17}$$

$$\text{Using} \quad w_i^p = \prod_{k=1}^{5} P_{ik}A_k^p(I_k^p); \quad \text{for} \quad \frac{\partial w_i^p}{\partial A_{km}^p} = P_{ik}\frac{\partial A_k^p}{\partial A_{km}^p}\prod_{K\neq k} P_{iK}A_K^p(I_K^p) \tag{18}$$

Finally, we can compute a partial derivative $\frac{\partial A_{km}^p}{\partial p_{km}}$ where $A_{km}^p(I_k^p) = ae^{-\frac{(I_k - \bar{I}_{km})^2}{2\sigma_{km}}}$; with respect to two parameters namely, $\bar{I}_k$ and σ_k taking care that the activation values should always be greater than zero. Thus, having obtained all the partial derivatives, we compute the chain rule mentioned in (15) and use it to update equation (14) to revise the parameters and reduce the error function. The results are shown in Figure 3. We are not optimizing the consequent variables in the fuzzy model, which we identify using pseudo-inverse of the previously obtained regressor matrix (11, 12).

The gradient descent approach that we describe here works iteratively in two stages: initially we perform the pseudo-inverse operation to identify the consequent variables for the initial assumed antecedent parameters and then we update the antecedent parameters using the error signal and the update equation (14). The expected value of the squared errors, E_p, decreases gradually with the number of iterations, reaching a minimum value of 4.3 within approximately 100 iterations. Further, Table 2 shows the values of vector, y_i after optimization, whereas the corresponding values of parameters B, C, and sigma are mentioned in Table 3.

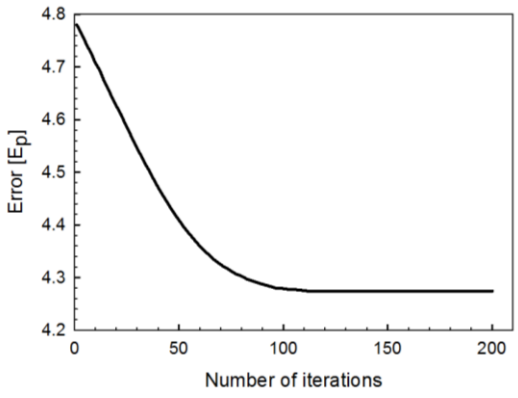

Figure 3: Minimization of expected value of the squared errors

Table 2: Vector of optimized consequent parameters (W) used in the fuzzy model for conversion prediction.

y_1	y_2	y_3	y_4	y_5	y_6	y_7	y_8
865172.0	-4372720	-117809.0	510856.0	-119494.0	574073.0	15231.11	-64196.02
y_9	y_{10}	y_{11}	y_{12}	y_{13}	y_{14}	y_{15}	y_{16}
64706.02	341811.8	4192.489	-8472.62	-2940.70	43662.40	8661.60	34265.87
y_{17}	y_{18}	y_{19}	y_{20}	y_{21}	y_{22}	y_{23}	y_{24}
-13166.55	-8997.181	489.3450	2049.933	-6313.479	193230.8	3220.417	-22374.79
y_{25}	y_{26}	y_{27}	y_{28}	y_{29}	y_{30}	y_{31}	y_{32}
12235.96	1252.068	1835.888	-9821.161	-30171.53	8724.090	4004.200	-6834.360

Table 3: Points of minimum fuzziness (*B & C in Figure 1*), and standard deviation (σ) before and after optimization, for all five variables.

Parameter	B		C		SIGMA	
	Initial values	After optimization	Initial values	After optimization	Initial values	After optimization
Concentration	01.71	00.33	03.04	03.74	00.80	00.62
Time	41.00	22.03	65.50	72.03	14.70	21.26
Temperature	103.75	75.01	151.25	159.00	28.50	35.68
L/S	08.96	01.26	16.98	19.97	04.81	07.99
Si/Al	01.85	01.33	02.74	02.79	00.53	00.82

Results and Discussion

We begin with the results of our experiments on synthesis of zeolites. As mentioned above, the parameters that were varied during synthesis of zeolite are concentration of alkaline solution, reaction time, temperature. Liquid to solid (L/S) was kept fixed at 20 ml/g and silica to alumina (Si/Al) ratio at 1.44 (the CFA samples collected in Astana, Kazakhstan has a Si/Al ratio of 1.44). The experiments were performed in duplicates and the reported conversion values are the average of two runs. The standard deviation between all the duplicate experiments was less than 5%. According to factorial analysis results, as shown in Table 4, if we consider the effect of one experimental parameter while keeping the others constant, it is obvious that the effect of reaction temperature and time is essential. In addition, we note that the effect of alkali concentration is minor compared to other parameters. When we consider the synergetic effect of two experimental parameters, we could observe a significant positive effect of temperature in combination with time and alkali concentration. However, the most noticeable positive effect in terms of conversion was observed when three experimental parameters were increased to highest values (within our experimental range).

Table 4: Parameters applied in production of synthetic zeolite from CFA based on factorial analysis. L/S = 20 ml/g and Si/Al = 1.44 are constant in all experiments. The conversion reported is an average of two runs.

#	# as in Table 1	Concentration (M)	Time (h)	Temperature (°C)	Conversion (%)	Factor(s) effect (%)
1	15	1	24	90	19.8	0
2	16	1	24	110	45.3	25.5
3	17	1	48	90	48.2	28.4
4	18	3	24	90	39.6	19.8
5	19	1	48	110	47.0	27.2
6	20	3	24	110	55.9	36.1
7	21	3	48	90	35.5	15.7
8	22	3	48	110	78.0	58.2

Further, the results for the fuzzy model and its optimization were mentioned in the previous sections along with the model for the ease of reader. Herein, we present the output of the model in comparison with the experimental values, followed by a discussion on effects of the parameters on zeolite formation. Figure 4 shows the percentage conversion to zeolites, for all 31 points as computed from the model, in comparison with the experimental values as noted in table 1. The output of model after optimization is found in close agreement with the experimental results. As noted above, points 15-22 are based on our experiments, whereas other observations are taken from the literature. Further, the percentage error between outputs from the experiments and the model are also shown in figure 4, wherein the average error is 4.7 % and the maximum error is 18.6 % for point 30.

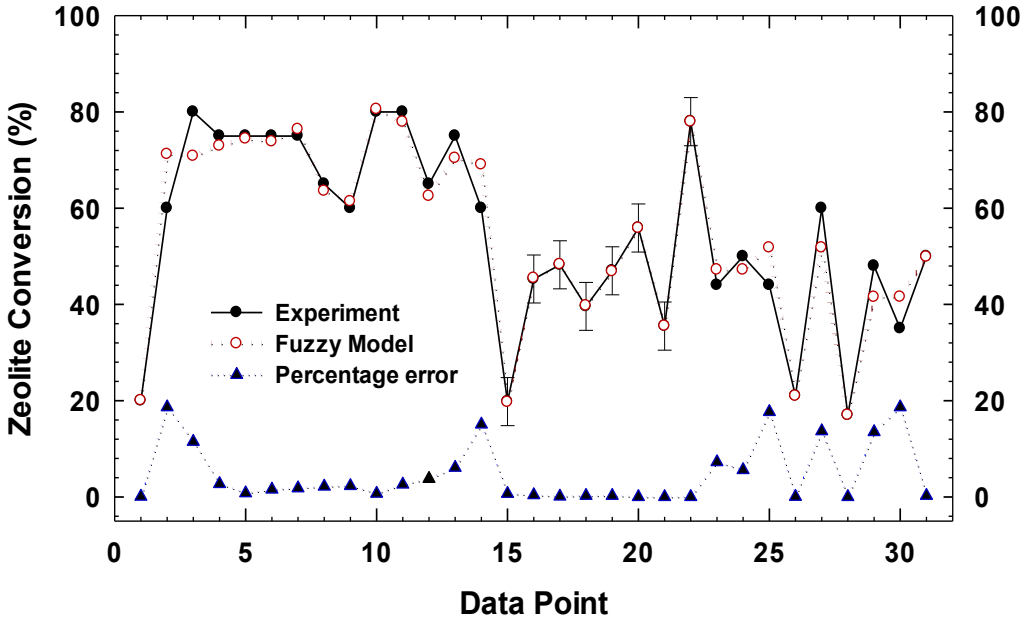

Figure 4: Zeolite conversion as obtained from the model in comparison with the experiments for all 31 data points as noted in Table 1. Points 15 to 22 are our experiments, with less than 5% standard deviation of error. Percentage error in predicting conversion using the fuzzy model is also shown.

Next, we discuss the effects of individual parameters, i.e., alkali concentration, time, temperature, L/S, and Si/Al on zeolite conversion. Taking into account the experimental results and the statistical data from literature on the effect of reaction parameters on conversion, we use the fuzzy model to analyze and investigate the effect of individual parameter on conversion. To this end, based on the model we systematically constructed dependence graphs by applying lowest, average, and highest values of parameters under study, while keeping the remaining parameters on their average values. For example, to see how the conversion changes with reaction time; concentration of alkali solution, reaction temperature, and L/S ratio were kept constant at their average values.

Figure 5 demonstrates the dependence of conversion on alkali concentration. In Figure 5a temperature was kept at 130 ^{o}C, time at 48 h, and L/S ratio at 10.625 ml/g, whereas in Figure 5b, the values were 117^{o}C, 48 h, and 20 ml/g, respectively. We also note in all the analysis mentioned below, Si/Al was kept fixed at 1.44, which is a constraint for our experiments, as mentioned above. From the figure, we observe that in both cases the conversion increases with concentration reaching a maximum value of 85% and 95%, respectively. It is interesting to note that the conversion is increased by 10% when the L/S ratio is changed from 10.625 to 20, while temperature is decreased from 130^{o}C to 117^{o}C. The pattern is probably due to change in the crystallinity of zeolites when the concentration of alkali solution is increased and the higher value of L/S creates the conditions for better reaction kinetics by forming more active sites to reach for Na^{+} ions to further form crystals.

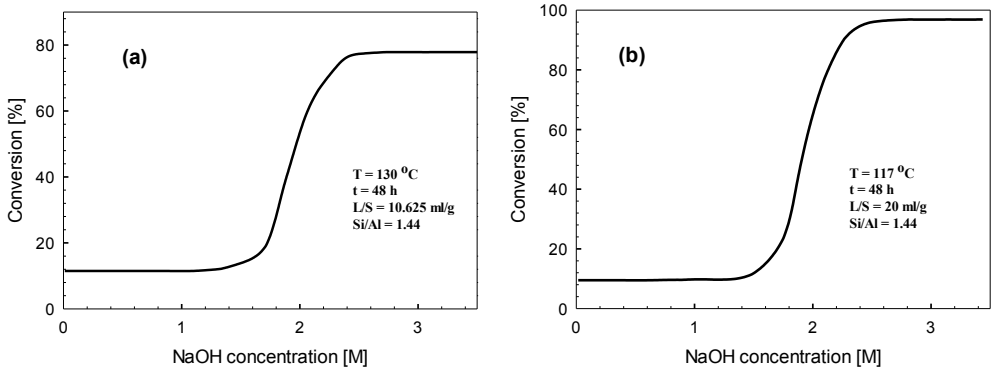

Figure 5: Dependence of conversion on alkali concentration as derived from the fuzzy model. The other parameters were (a) t = 48 h, T = 130 ^{o}C, L/S = 10.625 ml/g, Si/Al = 1.44 and (b) t = 48 h, T = 117 ^{o}C, L/S = 20 ml/g, Si/Al = 1.44

Further, as shown in Figure 6a and b, we clearly see the positive effect of reaction time, which is also confirmed from our experimental findings. Once again, the other parameters were kept constant at their average values. The modelling results reveal that over time the conversion gradually increases and reaches around 60% and 80%, correspondingly. It should also be noted that

when the reaction temperature is increased from 75 ºC to 117 ºC, the conversion obtained from our model is significantly raised by 20%. This pattern is also observed in in our experiments, where the effect of reaction temperature was the highest amongst others. The reason why the conversion increases over time and temperature could be explained by the fact that the crystal formation is a direct function of time: the more we allow crystals to grow, the higher the conversion [33]. Although, the alkali concentration is high in Figure 6b, we see that the effect of this parameter is relatively close to 0.5 M in terms of factorial analysis. We also see in figure 5 that, the *transition point*, i.e. the beginning of the curvature in the sigmoidal graph, is around 2 M, indicating that at concentrations less than 2 M, conversion does not depend on alkali concentrations. Figure 6c, further confirms the experimental results and hypothesis that when the L/S ratio is decreased, it reversely affects the conversion because less active sites are available for reaction to occur and for crystals to form and grow (conversion drops by approximately 15%).

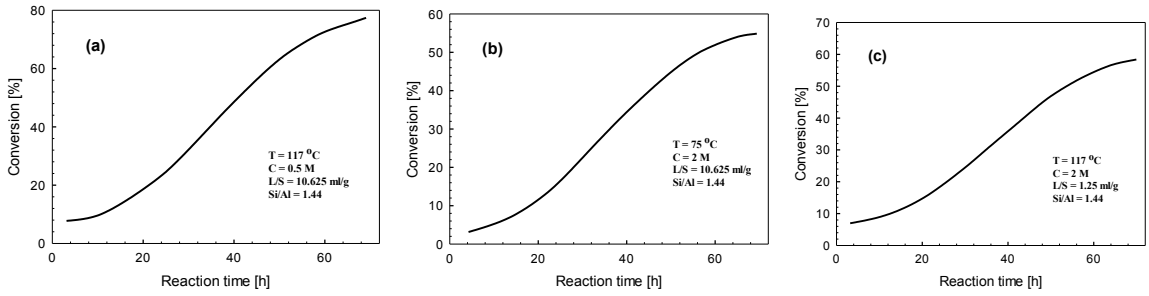

Figure 6: Dependence of conversion on reaction time. The other parameters were (a) T = 117 ºC, C = 0.5 M, L/S = 10.625 ml/g, (b) T = 75 ºC, C = 2M, L/S = 10.625 ml/g, and (c) T = 117 ºC, C = 2 M, L/S = 1.25 ml/g

Similarly, the reaction temperature positively affects the kinetics of synthesis, which in turn leads to production of more crystal phases that are the building blocks of zeolites as opposed to mainly amorphous CFA (See figure 7a and b). Although a constraint for us in our experiments, we

also analyze the effect of Si/Al ratio on conversion. As known from literature (See Garcia G., et al. [34, 35]), a high Si content in raw CFA accelerates the formation of crystalline phase, which in turn results in high synthesis of zeolites upon annealing at elevated temperature under appropriate alkaline environment. Comparing the figure 7a and b, we observe that even at relatively low change in Si/Al (from 1.29 to 1.44), an essential positive effect on conversion is observed, with about 22% increase in conversion. In addition, Figure 8 demonstrates the effect of L/S ratio on the conversion wherein a stepwise upward trend towards higher L/S ratio, as expected and explained above.

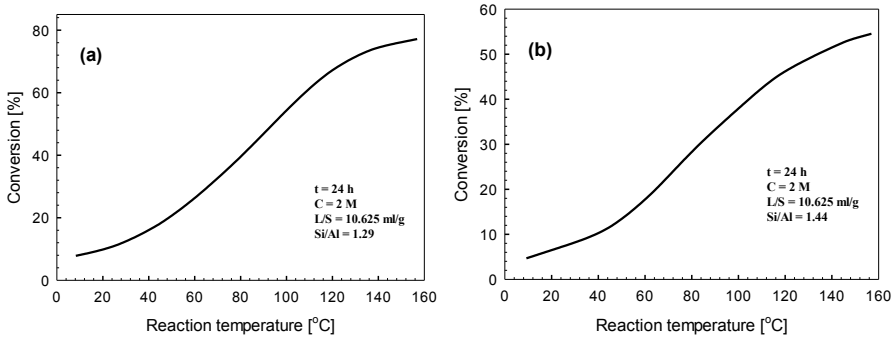

Figure 7: Dependence of conversion on reaction temperature, with a change in Si/Al. The other parameters were (a) t = 24 h, C = 2.0 M, L/S = 10.625 ml/g, Si/Al = 1.29 and (b) t = 24 h, C = 2.0 M, L/S = 10.625 ml/g, Si/Al = 1.44.

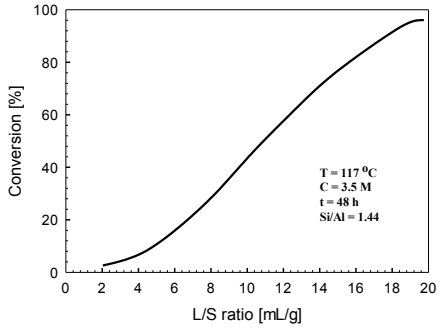

Figure 8: Dependence of conversion on L/S. The other parameters were C = 3.5 M, t = 48 h, T = 117 °C, Si/Al = 1.44

Conclusion

The work presented herein provides experimental results on the synthesis of zeolites from CFA under various reaction parameters, such as time, temperature, alkali concentration, Si/Al and L/S ratio. Depending on reaction parameters, an average conversion of CFA into synthetic zeolite, both in literature and our experiments, varies from ~20 to ~80%. The experimental results and literature data from two other sources were further investigated using heuristic approach in order to optimize the system identification of conversion. According to our findings, the optimized fuzzy models demonstrate an accurate correlation with average deviation of 5%, both with experimental results and literature values. These enable to conclude the possibility of use of heuristic approach with fuzzy models in conversion of CFA into zeolites, which allows predicting the effect of reaction parameters and guide on the possible formation mechanism of zeolite.

References:

1. Blissett, R.S. and N.A. Rowson, *A review of the multi-component utilisation of coal fly ash.* Fuel, 2012. **97**: p. 1-23.
2. Bukhari, S.S., et al., *Conversion of coal fly ash to zeolite utilizing microwave and ultrasound energies: A review.* Fuel, 2015. **140**: p. 250-266.
3. Delkash, M., B. Ebrazi Bakhshayesh, and H. Kazemian, *Using zeolitic adsorbents to cleanup special wastewater streams: A review.* Microporous and Mesoporous Materials, 2015. **214**: p. 224-241.
4. Aldahri, T., et al., *Synthesis of zeolite Na-P from coal fly ash by thermo-sonochemical treatment.* Fuel, 2016. **182**: p. 494-501.
5. Behin, J., et al., *Developing a zero liquid discharge process for zeolitization of coal fly ash to synthetic NaP zeolite.* Fuel, 2016. **171**: p. 195-202.
6. Ojumu, T.V., P.W. Du Plessis, and L.F. Petrik, *Synthesis of zeolite A from coal fly ash using ultrasonic treatment – A replacement for fusion step.* Ultrasonics Sonochemistry, 2016. **31**: p. 342-349.
7. Visa, M., *Synthesis and characterization of new zeolite materials obtained from fly ash for heavy metals removal in advanced wastewater treatment.* Powder Technology, 2016. **294**: p. 338-347.

8. Wang, J., et al., *Supercritical hydrothermal synthesis of zeolites from coal fly ash for mercury removal from coal derived gas.* Fuel Processing Technology, 2015. **136**: p. 96-105.
9. El-Mekkawi, D.M. and M.M. Selim, *Effect of metal loading processes on the stability and thermal transformation of Co2 +- and Cu2 +-zeolite Y prepared from Egyptian kaolin.* Materials Characterization, 2012. **69**: p. 37-44.
10. Ma, Y., et al., *Synthesis and characterization of 13X zeolite from low-grade natural kaolin.* Advanced Powder Technology, 2014. **25**(2): p. 495-499.
11. Maia, A.Á.B., et al., *Synthesis, optimisation and characterisation of the zeolite NaA using kaolin waste from the Amazon Region. Production of Zeolites KA, MgA and CaA.* Applied Clay Science, 2015. **108**: p. 55-60.
12. Liu, H., et al., *From natural aluminosilicate minerals to zeolites: synthesis of ZSM-5 from rectorites activated via different methods.* Applied Clay Science, 2015. **115**: p. 201-211.
13. Wdowin, M., et al., *The conversion technology of fly ash into zeolites.* Clean Technologies and Environmental Policy, 2014. **16**(6): p. 1217-1223.
14. Moriyama, R., et al., *Large-scale synthesis of artificial zeolite from coal fly ash with a small charge of alkaline solution.* Fuel, 2005. **84**(12–13): p. 1455-1461.
15. Querol, X., et al., *Synthesis of zeolites from fly ash at pilot plant scale. Examples of potential applications.* Fuel, 2001. **80**(6): p. 857-865.
16. Belviso, C., et al., *Removal of Mn from aqueous solution using fly ash and its hydrothermal synthetic zeolite.* Journal of Environmental Management, 2014. **137**: p. 16-22.
17. Wang, C., et al., *Evaluation of zeolites synthesized from fly ash as potential adsorbents for wastewater containing heavy metals.* Journal of Environmental Sciences, 2009. **21**(1): p. 127-136.
18. Bukhari, S.S., S. Rohani, and H. Kazemian, *Effect of ultrasound energy on the zeolitization of chemical extracts from fused coal fly ash.* Ultrasonics Sonochemistry, 2016. **28**: p. 47-53.
19. Musyoka, N.M., et al., *In situ ultrasonic monitoring of zeolite A crystallization from coal fly ash.* Catalysis Today, 2012. **190**(1): p. 38-46.
20. Molina, A. and C. Poole, *A comparative study using two methods to produce zeolites from fly ash.* Minerals Engineering, 2004. **17**(2): p. 167-173.
21. Shigemoto, N., H. Hayashi, and K. Miyaura, *Selective formation of Na-X zeolite from coal fly ash by fusion with sodium hydroxide prior to hydrothermal reaction.* Journal of Materials Science, 1993. **28**(17): p. 4781-4786.
22. Deng, H. and Y. Ge, *Formation of NaP zeolite from fused fly ash for the removal of Cu(ii) by an improved hydrothermal method.* RSC Advances, 2015. **5**(12): p. 9180-9188.
23. Xiao, M., et al., *Solid transformation synthesis of zeolites from fly ash.* RSC Advances, 2015. **5**(122): p. 100743-100749.
24. Choi, C.L., et al., *Salt-Thermal Zeolitization of Fly Ash.* Environmental Science & Technology, 2001. **35**(13): p. 2812-2816.
25. Liu, H., et al., *Magnetic zeolite NaA: Synthesis, characterization based on metakaolin and its application for the removal of Cu2+, Pb2+.* Chemosphere, 2013. **91**(11): p. 1539-1546.
26. Querol, X., et al., *Synthesis of zeolites from coal fly ash: an overview.* International Journal of Coal Geology, 2002. **50**(1–4): p. 413-423.
27. Cardoso, A.M., et al., *Synthesis of zeolite Na-P1 under mild conditions using Brazilian coal fly ash and its application in wastewater treatment.* Fuel, 2015. **139**: p. 59-67.
28. Luo, J., H. Zhang, and J. Yang, *Hydrothermal Synthesis of Sodalite on Alkali-Activated Coal Fly Ash for Removal of Lead Ions.* Procedia Environmental Sciences, 2016. **31**: p. 605-614.

29. Wang, Y., et al., *Synthesis of zeolites using fly ash and their application in removing heavy metals from waters*. Science in China, 2003. **46**(9): p. 967-976.
30. Derkowski, A., et al., *Properties and potential applications of zeolitic materials produced from fly ash using simple method of synthesis*. Powder Technology, 2006. **166**: p. 47-54.
31. Takagi, T. and M. Sugeno, *Fuzzy Identification on Systems and its Applications to Modeling and Control.* IEEE Trans. on Systems, Man, and Cybernatics, 1985. **15**: p. 116-132.
32. Pratihar, D.K., *Soft Computing*, 2008, Alpha Science International Ltd: Oxford.
33. Zhou S., et al., *Effects of the crystallization time on the synthesis of zeolite with flower-shaped crystals*. Materials Letters, 2015. **143**: p. 216-264
34. Garcia G., et al., *Synthesis of zeolite Y from diatomite as silica source*. Microporous and Mesoporous Materials, 2016. **219**: p. 29-37.
35. Sharma P., et al., *Synthesis of zeolite Y from diatomite as silica sourceInfluence of silica precursors on octahedron shaped nano NaY zeolite crystal synthesis*. Journal of the Taiwan Institute of Chemical Engineers, 2015. **50**: p. 259-265.